Title

Does dual-energy CT of lower-extremity tendons incur penalties in patient radiation exposure or reduced multiplanar reconstruction image quality?

Journal

American Journal of Roentgenology, 191(5)

ISSN

0361-803X

Authors

Lohan, Derek G
Motamedi, Kambiz
Chow, Kira
et al.

Publication Date

2008-11-01

DOI

10.2214/ajr.07.3624

Peer reviewed

Does Dual-Energy CT of Lower-Extremity Tendons Incur Penalties in Patient Radiation Exposure or Reduced Multiplanar Reconstruction Image Quality?

Derek G. Lohan[1]
Kambiz Motamedi
Kira Chow
Reza Habibi
Christoph Panknin
Stefan G. Ruehm
Leanne L. Seeger

OBJECTIVE. The purposes of this study were to evaluate the quality and radiation exposure of data acquired with dual-energy CT compared with single-energy MDCT in the depiction of lower-extremity tendons and to assess whether a dual-energy CT voltage exists at which the quality of tendon depiction is optimal.

SUBJECTS AND METHODS. Eleven healthy volunteers and seven clinically referred patients (10 men, eight women; mean age, 43.1 years; range, 20–71 years) underwent conventional single-energy CT and dual-energy CT examinations of both lower extremities with a dual-source CT scanner. Dual-energy reconstructions were made at combined tube voltages approximating 86, 98, 110, 122, and 134 kVp. Quantitative and qualitative analyses were performed on six tendons in each lower extremity, and the findings were compared with single-energy CT findings. The radiation dose involved was recorded in each case.

RESULTS. A trend toward increasing tendon attenuation was observed with increasing reconstructed tube voltage. The group of single-energy CT reconstructions proved significantly superior to each of the dual-energy CT reconstructions with regard to signal-to-noise ratio ($F = 35.25$, $p < 0.0001$) and contrast-to-noise ratio ($F = 37.19$, $p < 0.0001$), although interobserver agreement in subjective ranking was poor. Dual-energy CT had a significantly higher radiation dose ($p < 0.05$) than single-energy CT.

CONCLUSION. Dual-energy CT of lower-extremity tendons, irrespective of the reconstruction tube voltage chosen, yields multiplanar reformations inferior to those of single-energy CT with regard to signal-to-noise and contrast-to-noise ratios while involving significantly escalated patient exposure to ionizing radiation. Whether the tissue-differentiating promise of dual-energy CT is realized in future studies and warrants such concessions remains to be seen.

Keywords: dual-energy CT, ionizing radiation, tendon

DOI:10.2214/AJR.07.3624

Received January 6, 2008; accepted after revision May 9, 2008.

C. Pankin is an employee of Siemens Medical Solutions.

[1]All authors: Department of Radiological Sciences, David Geffen School of Medicine, University of California, Los Angeles, Medical Plaza 200, Ste. 165-59, Los Angeles, CA 90095. Address correspondence to D. G. Lohan (Derek.lohan@gmail.com).

AJR 2008; 191:1386–1390

0361–803X/08/1915–1386

The introduction of dual-source CT, which incorporates two orthogonally mounted tube–detector pairs within a single gantry [1], has had considerable implications with regard to coronary imaging, in which improved temporal resolution and avoidance of cardiac motion artifacts are paramount [2, 3]. The configuration of this CT system also offers the opportunity for dual-energy CT, whereby perfectly registered although independent helical data acquisition is achieved while the two CT tubes operate at energies of 80 and 140 kVp. Dual-energy CT is based on the principle that materials of unequal composition behave differently when exposed to varying x-ray spectra, manifesting as alterations in their attenuation values. The data obtained may be manipulated to display the specific attenuation responses of differing tissues. Such variations in attenuation may be significant for atoms with larger atomic numbers, such as iodine [4], an attribute that is the basis of much exploitation in contrast-enhanced vascular imaging. Only modest changes in attenuation are seen for collagenous structures, however, which consist mainly of the smaller atoms hydrogen, carbon, nitrogen, and oxygen. One such collagenous tissue is tendon, and conventional single-energy CT has a limited role in the diagnostic evaluation of this tissue.

Little evidence of the feasibility of dual-energy CT in the evaluation of tendinous continuity and integrity exists in the literature. A report by Johnson et al. [5] suggested that dual-energy CT is not associated with marked increases in ionizing radiation exposure of

patients. But what might dual-energy CT have to offer in imaging of lower-extremity tendons? Because the attenuation responses of various tissues differ, dual-energy CT should, at least in theory, enable isolated depiction of tendons without interference from adjacent soft tissues. In the presence of trauma, which results in peritendinous edema, dual-energy CT, owing to confident separation of tendon from adjacent fat stranding, may be useful for evaluation of the integrity of tendon. Similar evaluation of isolated tendon may be possible in the presence of degenerative tenosynovitis, in which separation of tendon from adjacent sheath fluid may not be possible with conventional CT. The utility of dual-energy CT in these roles remains to be proved.

Even if dual-energy reconstructions prove useful in clinical practice, diagnostic interpretation of dual-energy CT scans will rest with the cross-sectional axial, sagittal, and coronal multiplanar reconstructions (MPRs) produced, as is the case with other 3D CT applications. Dual-energy CT is unique in that once the data have been obtained, retrospective reconstruction can be achieved at any desired combined tube voltage between 80 and 140 kVp, allowing optimization of tube voltage to suit the tissue of greatest interest without repeated patient scanning.

We hypothesize that dual-energy CT is inferior to single-energy CT with regard to diagnostic quality of MPRs in tendon evaluation and that it results in higher radiation exposure. The basis for this hypothesis is that according to the fundamentals of radiation physics, image contrast is reduced with increasing tube voltage. As a result, one can expect the contrast-to-noise ratio (CNR) to be lower for dual-energy CT examinations, which involve at least a partial contribution from a CT tube operated at 140 kVp, compared with single-energy CT, which is performed at 120 kVp. Similarly for signal-to-noise ratio (SNR), a greater proportion of photon–tissue interactions occur in the form of coherent scatter rather than the photoelectric effect with increasing tube voltage. The result is a decrease in SNR at 140 kVp compared with 120 kVp, although one would expect this effect to be offset at least in part by relatively low noise from the 80-kVp tube–detector pair.

To establish an optimal voltage at which MPRs should be evaluated for diagnostic interpretation, should our hypothesis be proven incorrect, we sought to evaluate whether any one particular combined reconstruction voltage is associated with superior tendon depiction on dual-energy CT MPRs. Should our hypothesis hold true, voltage determination will represent a considerable obstacle to the future study and implementation of dual-energy CT, such use depending on the tissue-differentiating capabilities of the technique.

Subjects and Methods

All examinations were HIPAA compliant, and the study received institutional review board approval. After giving informed consent, 11 healthy volunteers and seven clinically referred patients (10 men, eight women; mean age, 43.1 years; range, 20–71 years) underwent conventional single-energy CT and then dual-energy CT of both lower extremities from the proximal tibial shaft to the distal phalanges on a dual-source CT system (Somatom Definition, Siemens Medical Solutions). The patients had been referred for osseous investigation related to trauma in four cases, suspected degenerative joint disease in two cases, and postoperative follow-up after resection of soft-tissue sarcoma in one case. The volume coverage used was chosen to include the area from the musculotendinous junctions to the insertion of the ankle joint tendons. The imaging parameters are shown in Table 1. An IV contrast agent was not administered in any case.

Initial processing was performed on the CT console with incorporated software. A fellowship-trained musculoskeletal radiologist with 7 years of experience was responsible for all data postprocessing. The raw data acquired at single-energy CT were reconstructed at 20-cm^2 field of view and 2-mm slice thickness at a 2-mm increments with a medium-smooth soft-tissue kernel (B30f). Processing of the dual-energy data involved integration of the data from each tube–detector pair, facilitating image reconstruction at any desired relative contribution of the low- and high-voltage tubes. Reconstructions were made at 20% intervals from 86 kVp (low voltage–to–high voltage ratio, 90%/10%) to 134 kVp (low voltage–to–high voltage ratio, 10%/90%), each 20% interval corresponding to an increase in mean voltage of approximately 12 kVp. Thus dual-energy reconstructions were performed at combined tube voltages approximating 86, 98, 110, 122, and 134 kVp. These data were reconstructed with a 20-cm^2 field of view and 2-mm slice thickness at 2-mm increments with a soft-tissue kernel (D30f) similar to that used for single-energy reformatting. No single kernel on the CT system was available for both single- and dual-energy CT reconstruction, so the most-similar soft-tissue kernels were used.

Quantitative Analysis

Evaluation of tendon attenuation focused on six tendons within various compartments of the ankle joint—the Achilles, tibialis posterior, flexor digitorum longus, flexor hallucis longus, peroneus longus, and tibialis anterior tendons. A region of interest was manually placed on each of these tendons at two locations, 5 cm and 1 cm proximal to the ankle joint, and the attenuation at each location was recorded. The region of interest measured was as large as possible but sufficiently small to avoid inclusion of adjacent fat and bone. Areas of beam hardening, found along the middle thirds of these structures because of their proximity to dense cortical bone, were intentionally avoided. The SD, which serves as a quantitative marker of the image noise for the surrounding air, and attenuation of the gastrocnemius muscle were measured in each case. The SNR and CNR for each tendon were calculated according to the following formulas:

$$\text{SNR} = \text{mean tendon attenuation} / \text{SD noise}_{(\text{air})}$$

$$\text{CNR} = (\text{mean tendon attenuation} - \text{gastrocnemius attenuation}) / \text{SD noise}_{(\text{air})}.$$

In all, these measurements were derived from six tendons on each side in 18 subjects at single-energy and at five separate dual-energy tube voltages (86, 98, 110, 122, and 134 kVp), for a total of 1,296 SNR and CNR values, which formed the basis of subsequent quantitative statistical analysis.

Qualitative Analysis

Two board-certified musculoskeletal radiologists, not including the radiologist responsible for data postprocessing, blinded to the method used for data acquisition, including the voltages of dual-energy examinations, performed an independent qualitative evaluation of the axial MPRs obtained in each case. Data sets were

TABLE 1: Single- and Dual-Energy CT Protocols

Parameter	Single Energy	Dual Energy
Tube voltage (kVp)	120	80, 140
Current (mA)	155	75, 320
Collimation (mm)	0.6	0.6
Pitch	0.9	0.9
Gantry rotation time (s)	1.0	0.5

TABLE 2: Mean Individual Tendon Attenuation Values Measured During Single-Energy CT and at Each Dual-Energy Reconstructed Tube Voltage

	Tendon					
Voltage (kVp)	Achilles	Tibialis Posterior	Flexor Digitorum Longus	Flexor Hallucis Longus	Peroneus Longus	Tibialis Anterior
Single-energy CT						
120	87.73	84.09	91.50	94.92	107.58	101.60
Dual-energy CT						
86	73.12	81.83	89.90	92.00	92.63	89.72
98	73.84	81.80	90.32	93.02	93.47	90.10
110	75.35	82.09	90.52	94.24	95.19	90.69
122	75.99	81.91	90.53	95.09	96.17	90.78
134	77.75	81.85	90.84	96.09	97.29	90.91

randomly presented in a 6 × 1 screen format, each with a 10 × 10 cm field-of-view, on a workstation (Wizard 3D, Siemens Medical Solutions). Each of the reconstructed data sets was subjectively ranked with regard to overall quality of tendon depiction from 1 (best) to 6 (worst), according to overall tendon conspicuity and edge definition. Allocation of joint ranks was permitted in the event of comparable image quality. Observers were requested to note artifacts identified in any data set, irrespective of cause.

Radiation Exposure

The effective dose to each subject was recorded from the scanner console for both the single- and dual-energy CT examinations in the form of CT dose index (CTDI) [6]. The volume CTDI, a derivative of the CTDI that can be used to express the average dose delivered to a scan volume for a specific examination, was recorded, as was the dose–length product.

Statistical Analysis

Statistical analysis was performed with Stata software (version 10.0, Stata). Repeated measures two-factor analysis of variance was used to evaluate for differences in SNR and CNR data obtained from the single-energy and each of the dual-energy reconstructions. A within-subject design was used to minimize the effect of intersubject variability. Friedman's nonparametric test was used to verify that any significant results obtained did not occur as a result of nonnormal distribution of data. The presence of significant interobserver difference between the ranks assigned to each reconstructed data set was evaluated with weighted kappa analysis, whereby a score of 1 was assigned for corresponding tendon scores and 0.5 to scores that differed by a single rank. Interobserver deviation of more than one rank was not assigned any score according to the weighting system used. A kappa value of 0 was taken as indicative of poor interobserver agreement; 0.01–0.20, slight agreement; 0.21–0.40, fair agreement; 0.41–0.60, moderate agreement; 0.61–0.80, good agreement; and 0.81–1.00, excellent agreement. Intrarater agreement was evaluated with the Cronbach alpha reliability coefficient. A paired Student's *t* test was used to evaluate for potential difference in the dose–length product measure of radiation exposure between single- and dual-energy examinations. A value of $p < 0.05$ was designated as representing statistical significance, prompting rejection of the null hypothesis.

TABLE 3: Calculated Mean Signal-to-Noise and Contrast-to-Noise Ratios for Single- and Dual-Energy CT Reconstructed Data Sets

	Single Energy	Dual Energy				
Ratio	120 kVp	86 kVp	98 kVp	110 kVp	122 kVp	134 kVp
Signal to noise	26.9 ± 6.6	20.4 ± 5.1	22.9 ± 6.6	23.2 ± 7.7	21.1 ± 8.2	17.7 ± 7.0
Contrast to noise	11.8 ± 4.6	8.3 ± 3.5	8.9 ± 4.0	8.6 ± 3.9	7.5 ± 3.7	6.1 ± 3.3

Note—Values are mean ± SD.

TABLE 4: Calculated Dose Values for Single- and Dual-Energy CT Protocols

Parameter	Single Energy	Dual Energy
Collimation (mm)	0.6	0.6
Pitch	0.9	0.9
Volume CT dose index, mean ± SD	11.4 ± 0.55	16.5 ± 2.9
Dose–length product, mean ± SD (mGy × cm)	435 ± 120	617 ± 257

Results

SNR and CNR Analysis

Table 2 shows the mean attenuation values of the individual tendons evaluated at each of the reconstructed dual-energy voltage values. The mean ± SD SNR and CNR for each of the reconstructed data sets is provided in Table 3. Each SNR and CNR measurement derived from the single-energy CT examinations proved superior to those obtained from each of the reconstructed dual-energy CT intervals to a statistically significant degree (SNR, $F = 35.25$, $p < 0.0001$; CNR, $F = 37.19$, $p < 0.0001$; analysis of variance).

Qualitative Analysis

Observer 1 designated the single-energy CT MPRs of superior image quality with a median ranked score of 1.0. For observer 2, the 134-kVp reconstructions were most consistently awarded the top ranking, for a median ranked score of 1.5. Weighted kappa analysis revealed a poor level of interobserver agreement between the two observers with regard to ranking of the various image data sets ($\kappa = 0.014$). Intrarater agreement was considerable for observer 1 ($\alpha = 0.85$) and less so for observer 2 ($\alpha = 0.56$, Cronbach alpha reliability coefficient).

Radiation Exposure

Calculated mean dose profiles for single- and dual-energy CT are shown in Table 4. A statistically significant difference between the techniques was observed with regard to both volume CTDI ($p = 0.004$) and dose–length product ($p = 0.003$).

Discussion

Our findings suggest that with regard to SNR and CNR, MPRs derived from

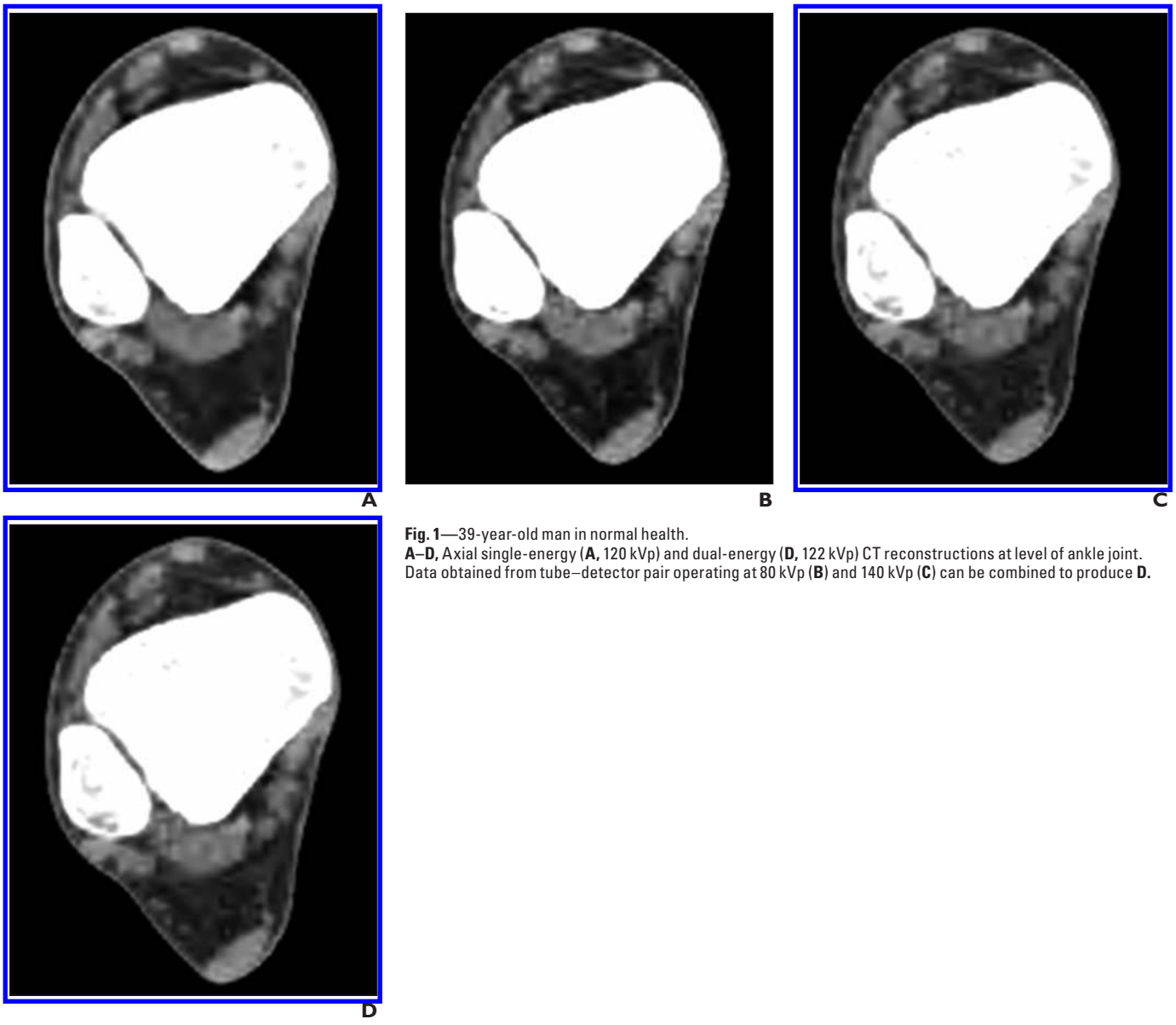

Fig. 1—39-year-old man in normal health.
A–D, Axial single-energy (**A,** 120 kVp) and dual-energy (**D,** 122 kVp) CT reconstructions at level of ankle joint. Data obtained from tube–detector pair operating at 80 kVp (**B**) and 140 kVp (**C**) can be combined to produce **D.**

dual-energy CT data, irrespective of the reconstructed combined tube voltage chosen, are inferior to those derived from single-energy CT data (Fig. 1). The level of statistical significance with regard to SNR and CNR surpasses that intuitively expected, given the mean and SD values in Table 3. Table 3, however, contains data comparable both within subjects and between subjects, rendering it more complex than suggested by the final numbers. This factor was taken into account in the statistical analysis, in which analysis of variance was performed with a within-subject design to partially rule out intersubject variability. This process allowed detection of true intraobserver differences in SNR and CNR with regard to single- and dual-energy CT techniques.

Although the clear objective superiority of single-energy CT was not indisputably found in the subjective analysis, one of the two observers did score preferentially in favor of this technique. Nonetheless, the poor interobserver agreement in ranks assigned ($\kappa = 0.014$) and the relative consistency with which the observers individually assigned their ranks ($\alpha = 0.85$ for observer 1, $\alpha = 0.56$ for observer 2) suggest that any subjective difference that might exist between single- and dual-energy CT data may be subtle. With regard to ionizing radiation, dual-energy CT was determined to involve significantly higher levels of exposure per helical rotation (volume CTDI, $p = 0.004$) than single-energy CT and as a function of the entire examination (dose–length product, $p = 0.003$).

Despite considerable relatively recent enthusiasm about potential clinical applications, implementation of dual-energy CT is entering its fourth decade [7, 8]. Early attempts at application of this technique were limited by a number of technical obstacles, including insufficient tube current, the resultant variations in attenuation values, prolonged imaging times, and the requirement for sequential rather than simultaneous scans for complete dual-energy

data acquisition [9–11]. The more recent past has seen remarkable developments in CT hardware and software, such that the versatility and implementation of this technique are now almost unrecognizable compared with those of its infancy [12]. It was, however, not until the introduction of dual-source CT in 2005 that application of these advances in dual-energy scanning rekindled interest in the technique. Because it allows simultaneous dual-energy MDCT data acquisition, dual-source CT addresses many of the limitations experienced in earlier attempts at application of the technique, facilitating the transition of dual-energy CT from theory to reality [1].

Early reports on the potential efficacy of the dual-energy approach focused on differentiation of iodine-based contrast medium–containing structures, such as vessels and enhanced viscera. This focus reflects the relatively exaggerated variation in attenuation values of high-atomic-number atoms, such as iodine, during imaging at varying tube voltages [5, 13]. The future of dual-energy CT is much less certain with regard to evaluation of collagenous tissues, such as tendon, in which relatively muted attenuation responses occur. In this study, during the transition from a dual-energy CT reconstruction voltage of 86 kVp to 134 kVp, the overall mean individual tendon attenuation variation was an increase of 2.49 HU (range, –14.2 to 20.6 HU), representing a mean increase in attenuation of 2.88% from baseline. This finding suggests that in the absence of marked alteration in composition, and thus attenuation response, of a particular tendon affected by a pathologic process, the role of dual-energy CT in the evaluation of lower-extremity tendons is far from certain.

There is little doubt that studies of the material-specific 3D applications of dual-energy CT will be performed in the near future, and the findings are eagerly awaited. Potential applications include isolated tendon depiction in the presence of trauma. In this use, differentiation of tendon from soft-tissue attenuation related to peritendinous edema or tenosynovitis may be possible, allowing confirmation of tendon integrity and identification of sites of tendinosis not otherwise appreciable with the limited contrast resolution of conventional single-energy CT. To our knowledge, there is no evidence to suggest that this technique is superior to single-energy CT for any of these applications. Our findings suggest that future studies should proceed with caution because use of the described dual-energy CT protocol necessitates concessions in image quality in the form of objective SNR and CNR and in patient exposure to ionizing radiation. Nonetheless, should such studies show a distinct diagnostic advantage of dual-energy CT over conventional single-energy CT in tendon analysis, particularly in patients for whom MRI is contraindicated (e.g., those with pacemakers or claustrophobia), the risk-to-benefit ratio may swing in the direction of the newer technique. In the absence of such contraindications, it is unlikely that dual-energy CT will challenge MRI, at least in its current form, as the reference standard technique for tendon evaluation.

We conclude that dual-energy CT of lower-extremity tendons, irrespective of the reconstruction voltage chosen, yields MPRs inferior to those obtained with single-energy CT with regard to SNR and CNR while entailing significantly escalated patient exposure to ionizing radiation. Whether the tissue-differentiating promise of dual-energy CT is realized in future studies and warrants the concessions remains to be seen. Such investigation should proceed with caution, however, in light of the findings of our study.

Acknowledgments

We thank Phil Ender, Xiao Chen, and Rose Medeiros, Statistical Consulting Group, UCLA Academic Technology Services, for their considerable input.

References

1. Flohr TG, McCollough CH, Bruder H, et al. First performance evaluation of a dual-source CT (DSCT) system. *Eur Radiol* 2006; 16:256–268
2. Johnson TR, Nikolaou K, Busch S, et al. Diagnostic accuracy of dual-source computed tomography in the diagnosis of coronary artery disease. *Invest Radiol* 2007; 42:684–691
3. Seifarth J, Wienbeck S, Pusken M, et al. Optimal systolic and diastolic reconstruction windows for coronary CT angiography using dual-source CT. *AJR* 2007; 189:1317–1323
4. Riederer SJ, Mistretta CA. Selective iodine imaging using k-edge energies in computerized x-ray tomography. *Med Phys* 1977; 4:474–481
5. Johnson TR, Krauss B, Sedlmair M, et al. Material differentiation by dual energy CT: initial experience. *Eur Radiol* 2007; 17:1510–1517
6. Shope TB, Gagne RM, Johnson GC. A method for describing the doses delivered by transmission x-ray computed tomography. *Med Phys* 1981; 8:488–495
7. Genant HK, Boyd D. Quantitative bone mineral analysis using dual energy computed tomography. *Invest Radiol* 1977; 12:545–551
8. Adams JE, Chen SZ, Adams PH, Isherwood I. Measurement of trabecular bone mineral by dual energy computed tomography. *J Comput Assist Tomogr* 1982; 6:601–607
9. Millner MR, McDavid WD, Waggener RG, Dennis MJ, Payne WH, Sank VJ. Extraction of information from CT scans at different energies. *Med Phys* 1979; 6:70–71
10. Dunscombe PB, Katz DE, Stacey AJ. Some practical aspects of dual-energy CT scanning. *Br J Radiol* 1984; 57:82–87
11. Mendler MH, Bouillet P, Le Sidaner A, et al. Dual-energy CT in the diagnosis and quantification of fatty liver: limited clinical value in comparison to ultrasound scan and single-energy CT, with special reference to iron overload. *J Hepatol* 1998; 28:785–794
12. Rubin GD. Data explosion: the challenge of multidetector-row CT. *Eur J Radiol* 2000; 36:74–80
13. Scheffel H, Stolzmann P, Frauenfelder T, et al. Dual-energy contrast-enhanced computed tomography for the detection of urinary stone disease. *Invest Radiol* 2007; 42:823–829

This article has been cited by:

1. Tyler M. Coupal, Paul I. Mallinson, Patrick McLaughlin, Savvas Nicolaou, Peter L. Munk, Hugue Ouellette. 2014. Peering through the glare: using dual-energy CT to overcome the problem of metal artefacts in bone radiology. *Skeletal Radiology* **43**, 567-575. [CrossRef]
2. Ralf G ThieleImaging of gout 96-107. [CrossRef]
3. Trenton D. Roth, Kenneth A. Buckwalter, Robert H. Choplin. 2013. Musculoskeletal Computed Tomography: Current Technology and Clinical Applications. *Seminars in Roentgenology* **48**, 126-139. [CrossRef]
4. S. Fickert, M. Niks, D. J. Dinter, M. Hammer, S. Weckbach, S. O. Schoenberg, L. Lehmann, S. Jochum. 2013. Assessment of the diagnostic value of dual-energy CT and MRI in the detection of iatrogenically induced injuries of anterior cruciate ligament in a porcine model. *Skeletal Radiology* **42**, 411-417. [CrossRef]
5. Savvakis Nicolaou, Teresa Liang, Darra T. Murphy, Jeff R. Korzan, Hugue Ouellette, Peter Munk. 2012. Dual-Energy CT: A Promising New Technique for Assessment of the Musculoskeletal System. *American Journal of Roentgenology* **199**:5_supplement, S78-S86. [Abstract] [Full Text] [PDF] [PDF Plus]
6. Ji Hoon Park, Se Hyung Kim, Hee Sun Park, Gi Hyeon Kim, Jae Young Lee, Jeong Min Lee, Joon Koo Han, Byung Ihn Choi. 2011. Added value of 80kVp images to averaged 120kVp images in the detection of hepatocellular carcinomas in liver transplantation candidates using dual-source dual-energy MDCT: Results of JAFROC analysis. *European Journal of Radiology* **80**, e76-e85. [CrossRef]
7. M. Cejna, A. Schuster, G. Heinzle. 2011. Schnittbilddiagnostik vor und nach Arthroskopie. *Arthroskopie* **24**, 95-102. [CrossRef]
8. Anja Apel, Joel G. Fletcher, Jeff L. Fidler, David M. Hough, Lifeng Yu, Luis S. Guimaraes, Matthias E. Bellemann, Cynthia H. McCollough, David R. Holmes, Christian D. Eusemann. 2011. Pilot multi-reader study demonstrating potential for dose reduction in dual energy hepatic CT using non-linear blending of mixed kV image datasets. *European Radiology* **21**, 644-652. [CrossRef]
9. B Gonzales, D Lalush. 2011. Full-Spectrum CT Reconstruction Using a Weighted Least Squares Algorithm With an Energy-Axis Penalty. *IEEE Transactions on Medical Imaging* **30**, 173-183. [CrossRef]
10. Christoph Thomas, Andreas Korn, Dominik Ketelsen, Soeren Danz, Ilias Tsifikas, Claus D. Claussen, Ulrike Ernemann, Martin Heuschmid. 2010. Automatic Lumen Segmentation in Calcified Plaques: Dual-Energy CT Versus Standard Reconstructions in Comparison With Digital Subtraction Angiography. *American Journal of Roentgenology* **194**:6, 1590-1595. [Abstract] [Full Text] [PDF] [PDF Plus]